Revista de Chimie
https://revistadechimie.ro
https://doi.org/10.37358/Rev.Chim.1949

Xanthan Matrix as Drug Delivery System

NARCIS ANGHEL*, MARIA VALENTINA DINU, FLORICA DOROFTEI, IULIANA SPIRIDON
"Petru Poni" Institute of Macromolecular Chemistry, 41 Grigore Ghica Voda Str., 700487 Iasi, Romania

***Abstract**: Here we present a new drug delivery system based on xanthan esterified with acrylic acid. This material served as a matrix for the incorporation of bioactive substances with antimicrobial and anti-inflammatory properties. The materials were characterized by Fourier Transform Infrared Spectroscopy (FTIR), Nuclear Magnetic Resonance (NMR) and Scanning Electron Micrography (SEM). Mechanical strength tests showed a substantial improvement in the resilience and flexibility of the polymer matrix modified by esterification under conditions of mechanical stress. The release of bioactive substances from the basic matrix follows a Korsmeyer-Peppas type kinetics. The modified xanthan-based transport system was shown to be antimicrobial active with an inhibition rate of almost 100% on gram-positive and gram-negative bacteria. The obtained results recommend this biomaterial for the manufacture of transdermal drug delivery devices.*

***Keywords**: xanthan, acrylic acid, amoxicillin, ketoprofen, drug delivery*

1. Introduction

The 21st century is certainly characterized by a truly technological advance. Characterized by an exponential evolution of hi-tech technologies, the development of new concepts and scientific theories with wide practical applications, it seems somewhat strange the reorientation towards the use, on an increasingly large scale, of natural polymeric materials in different fields of activity that interfere with the biological sphere.

Obviously, natural polymers (e.g. cellulose, chitosan, dextran, pullulan, alginate, xanthan, etc.) present a much more attractive alternative compared to synthetic ones, here referring to bioavailability, biocompatibility and biodegradability [1]. However, their number is somewhat small but the possibilities to manipulate their properties through appropriate chemical modifications are much higher. Of all these natural polymers, a special category is represented by those that are soluble in water and that have the capacity to modify the properties of the environment in which they are introduced by the ability to swell, thicken or form gels or films. Of all these polysaccharides, xanthan seems to be the optimal candidate for food, cosmetic and pharmaceutical applications.

Xanthan is produced, on an industrial scale, by the fermentation of simple sugars under the action of the bacterium *Xanthomonas campestris*, hence its generic name.

Xanthan is an anionic polysaccharide composed of a β-(1→4)-D-glucopyranose frame with side chains of (1→3)-α-D-mannopyranose-(2→1)-β-D-glucuronic acid-(4→1)-β-D-mannopyranose. The terminal mannose residues are about half 4,6-pyruvated. The mannose residues from the core matrix are almost 6-acetylated. Its properties make it a precious component for drug delivery systems.

From this point of view, xanthan has found medical applications such as implants [2,3], topical applications [4–8] or drug release systems [9–12].

At the same time, this biopolymer is known for its bioadhesiveness, which makes it adherent to the site of its application, thus having a pronounced effect on the healing of any skin wounds [13,14].

From the above, xanthan is erected as a natural material that has multiple valences that have found use in a wide range of practical applications. But we must keep in mind that it does not have an inherent mechanical strength, which does not make it suitable for the manufacture of devices or materials that require such a feature.

**email: anghel.narcis@icmpp.ro*

Moreover, the development of mechanically resistant, elastic systems with good bioadhesiveness, suitable for the design of devices for the release of bioactive substances in topical skin applications, requires careful modification of this polysaccharide. Here we refer to the fact that, given the hydrophilicity of this polymer, it must be somewhat modified so that in contact with a humid environment the supramolecular edifice of the material does not crumble.

One way to develop such systems that involve minimal, economically feasible changes implies the introduction of chemical functions that give rise to the establishment of hydrophobic bonds between polysaccharide macromolecules [15–17].

Given the above, the aim of this study was to create a new formulation, based on the chemical modification of xanthan by esterification with acrylic acid, of a delayed release system of a combination of amoxicillin / ketoprofen with possible uses in the topical application on the skin of patches with antimicrobial and anti-inflammatory action.

2. Materials and methods

2.1. Materials

Xanthan (M_w= 2.5 ×10^6 Da) from *Xanthomonas campestris*, Pluronic F-127, 4-toluenesulfonyl chloride (TsCl), pyridine (Py), dicyclohexylcarbodiimide (DCC), methylene chloride, amoxicillin, ketoprofen and human albumin were from Sigma-Aldrich (USA); acrylic acid was from Merck & Co. (USA).

2.2. Synthesis of xanthan acrylate

Esterification of xanthan with acrylic acid (Figure 1), in order to introduce double bonds capable of establishing hydrophobic interactions, was performed by two methods. The former used DCC (dicyclohexylcarbodiimide) as a coupling agent, but the removal of the by-product (dicyclohexylurea) proved to be very difficult and practically unfeasible. The second method used as an intermediate the tosylate of acrylic acid which proved to be a viable way both as reaction conditions and as ease of separation and purification of the final product (Scheme1) by an adapted strategy described by Sahoo et al [18].

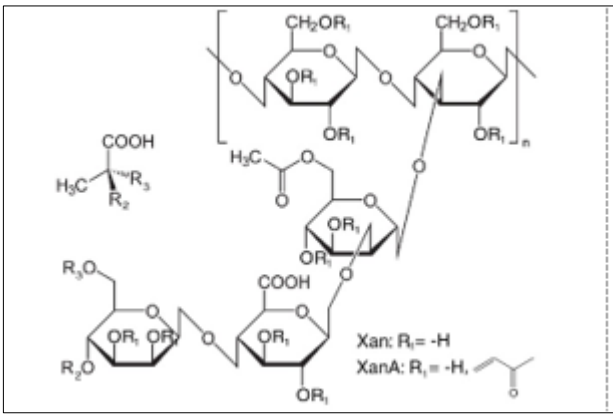

Figure 1. Chemical structure of xanthan (Xan) and xanthan acrylate (XanA)

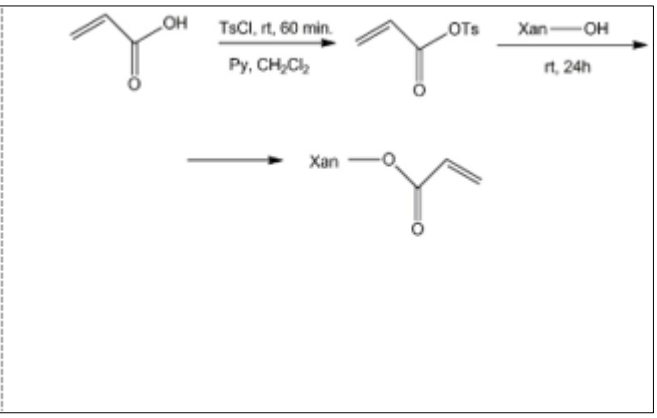

Scheme 1. Synthetic route for esterification of xanthan with acrylic acid

5.1 g TsCl (0.0267 mol), 6 mL pyridine (0.154 mol) and 1.9 mL (0.0267 mol) acrylic acid in 100 mL methylene chloride are placed in a round bottom flask equipped with a magnetic stirrer. The mixture is kept under stirring at room temperature for 60 min. The resulted by-product, pyridine hydrochloride, is removed by filtration. 10 g of xanthan (0.107 mol) are added to the filtrate thus obtained and the mixture is stirred for 24 h at room temperature. Reaction product was separated by filtration and wash on the filter with methylene chloride (pyridine, toluene sulfonic acid and Py·TsOH are soluble in methylene

chloride) and ethanol, after which it is dried at room temperature. The product comes in a yellowish-white, odorless and tasteless powder. Yield 9.91g.

The esterification process proceeds somewhat selectively at the primary hydroxyl groups, not excluding the participation of a certain proportion of the secondary alcohol groups present in the structure of xanthan.

2.3. Encapsulation of drugs into xanthan matrix

500 mg polysaccharide and 50 mg Pluronic F-127 (porosity control agent) are transferred to a Berzelius beaker containing 100 mL of distilled water. The mixture is stirred at 50°C for about 120 min. A first film was cast and dried at room temperature. 60 mg of a 2: 1 amoxicillin / ketoprofen mixture is added to the film thus obtained, over which a new layer of polysaccharide is poured. Thus, capsules with a core containing a broad-spectrum antibiotic plus a nonsteroidal anti-inflammatory are obtained. They were generically named XanAK and XanAAK after the type of polysaccharide used, non-modified or chemically modified, respectively.

2.4. *In vitro* drug release

In vitro release of amoxicillin and ketoprofen was carried out in phosphate buffer solution (pH 7) at 37 °C. Sample materials (XanAK and XanAAK), each containing 40 mg amoxicillin and 20 mg ketoprofen were immersed in 50 mL phosphate buffer solution. Aliquots of 1.5 mL were removed at different time intervals for about 140 min and readings were performed simultaneously at 240 and 254 nm for ketoprofen and amoxicillin respectively, using an UV-Vis spectrophotometer. Concentration of drugs was determined based on calibration curves.

2.5. FTIR (Fourier Transform Infrared spectroscopy) analysis

FTIR spectra of the composite materials were recorded using a Vertex 70FTIR spectrometer from Brüker (Billerica, MA, USA), equipped with an ATR device (ZnSe crystal) with a 45 angle of incidence. 64 scans were acquired with a spectral resolution of 2 cm^{-1}.

2.6. UV-VIS spectroscopy

UV-VIS measurements were performed on a Jenway 6450 spectrophotometer (Cole-Parmer, Staffordshire, UK) with the ability to read at two wavelengths simultaneously.

2.7. ^{1}H-NMR (Proton Nuclear Magnetic Resonance) analysis

The NMR spectra were recorded on a Brüker Avance DRX 400 MHz spectrometer (Germany). NMR spectra were obtained in D_2O solution.

2.8. Evaluation of *in vitro* anti-inflammatory activity

Anti-inflammatory activity of samples was estimated by albumin denaturation method [19–22]. Ketoprofen drug was used as standard. The reaction mixture consists of XanAK, XanAAK patches, or standard ketoprofen (20mg) in 15 mL saline phosphate buffer (pH-6.4) of 0.1% solution of human albumin. The reaction mixture was incubated at 27 °C for 60 min. Denaturation was induced by keeping the reaction mixture at 70 °C in a water bath for 10 min. After cooling, the absorbance was read at 660 nm using distilled water as blank. Each experiment was done in triplicate and the anti-inflammatory capacity was calculated as inhibition percent as follows:

$$Inhibition\ (\%) = \frac{OD_{sample} - OD_{control}}{OD_{control}} \quad (1)$$

where OD is optical density at 660 nm.

2.9. Antimicrobial activity

Candida albicans (ATCC 90028), *Staphylococcus aureus* (ATCC 25923) and *Escherichia coli* (ATCC 2592) were used to assess the antimicrobial activity of the materials.

2.10. Scanning Electron Microscopy (SEM)

The images were taken at a magnification of 5000 × using a VEGA TESCAN microscope (TESCAN ORSAY, Brno – Kohoutovice, Czech Republic), at an acceleration voltage of 20 kV. Prior to the SEM investigation, the fractured surfaces of the impact test specimens were sputtered with gold.

2.11. Mechanical measurements

The compressive properties of Xan-based hydrogel films were evaluated by a Shimadzu Testing Machine EZTest (Shimadzu Corporation, Japan) at 22°C using a crosshead speed of 1 mm min^{-1}. The swollen samples, as plate form with a thickness, width, and height of about 12 mm, 14 mm, and 3 mm, respectively, were uniaxial compressed using a maximum loading capacity of 100 N. The values of elastic modulus were quantified according to the procedure already reported for other polysaccharide-based hydrogels [23].

3. Results and discussions

3.1. FTIR analysis

FTIR measurements were performed in order to investigate the presence of acrylate moiety in the chemically modified xanthan. The FTIR spectra of materials are presented in Figure 2.

First, there is a decrease in the band intensity characteristic for the hydroxyl groups to 3360 cm^{-1} and an intensification of the stretching vibrations of the –CH_2– groups to 2920 cm^{-1} for XanA (Figure 2b). This, corroborated with the intensification of the absorption band of the carbonyl group at 1720 cm^{-1}, suggests the introduction of new ester groups in the structure of xanthan. Presence of double bond was confirmed by peaks at 1627, 1488 cm^{-1} for stretching, and bending at vibrations 919 cm^{-1}.

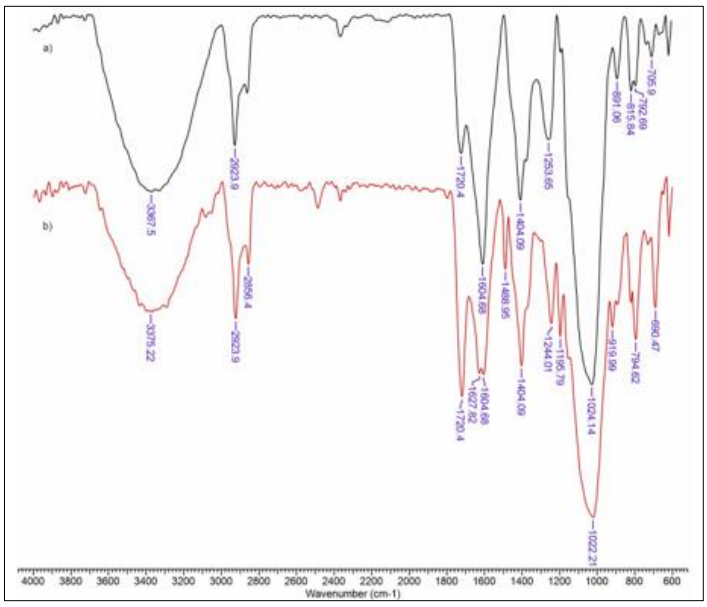

Figure 2. FTIR spectra for Xan (a) and XanA (b)

3.2. NMR characterization

The ^{1}H-NMR spectra for xanthan is given in Figure 3a. Peak at 1.2 ppm is attributed to the pyruvate methylene(-CH_3). The signal at 2.09 ppm corresponds to methyl protons of acetate moiety in the side chain of xanthan. Multiple signals at 3.0–4.0 ppm are related to protons of alcoholic (–CH–OH) and (–CH_2–OH) motifs in xanthan structure. The equatorial anomeric proton, H-l-alpha, of mannopyranosic

unit C, which is known as the more deshielded proton is located at 5.2 ppm [24]. These findings are in agreement with NMR spectra recorded for xanthan [25–28].

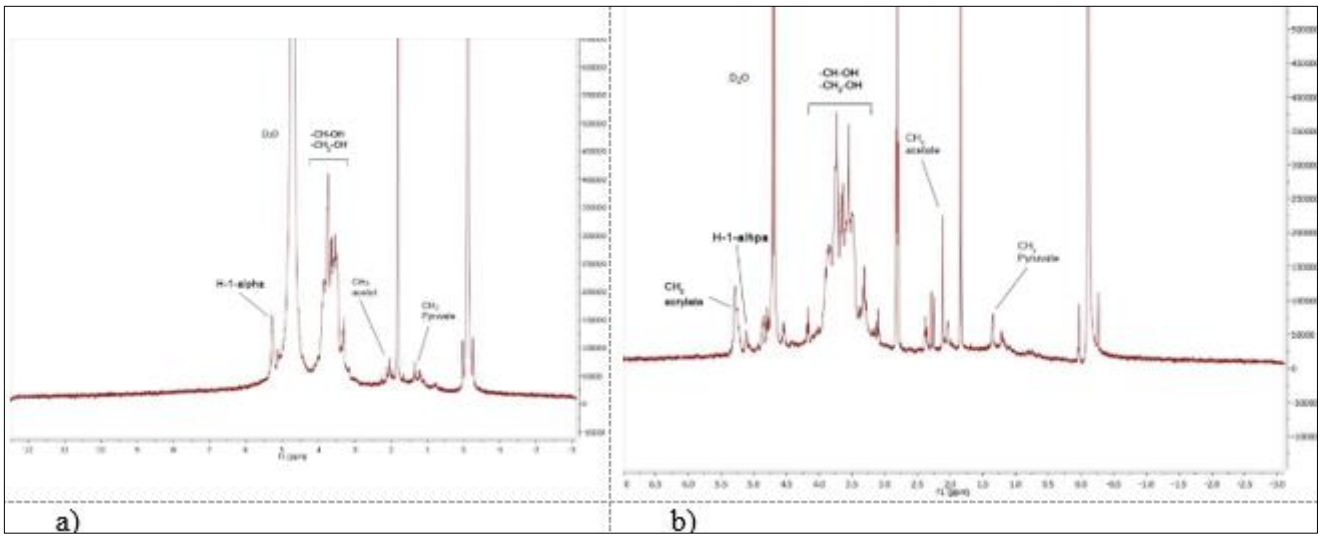

Figure 3. ^{1}H-NMR spectra for Xan (a) and XanA (b)

The evidence that the acrylic acid esterification reaction took place is given by the NMR spectrum of the modified xanthan in Figure 3b. The appearance of a signal at 5.5 ppm, characteristic for beta protons of the acrylic group, supports this statement, according to literature data [29,30].

3.3. Mechanical properties

The compression stress-strain measurements were performed on swollen Xan hydrogel films as well as on XanAK and XanAAK patches and the data obtained are summarized in Figure 4.

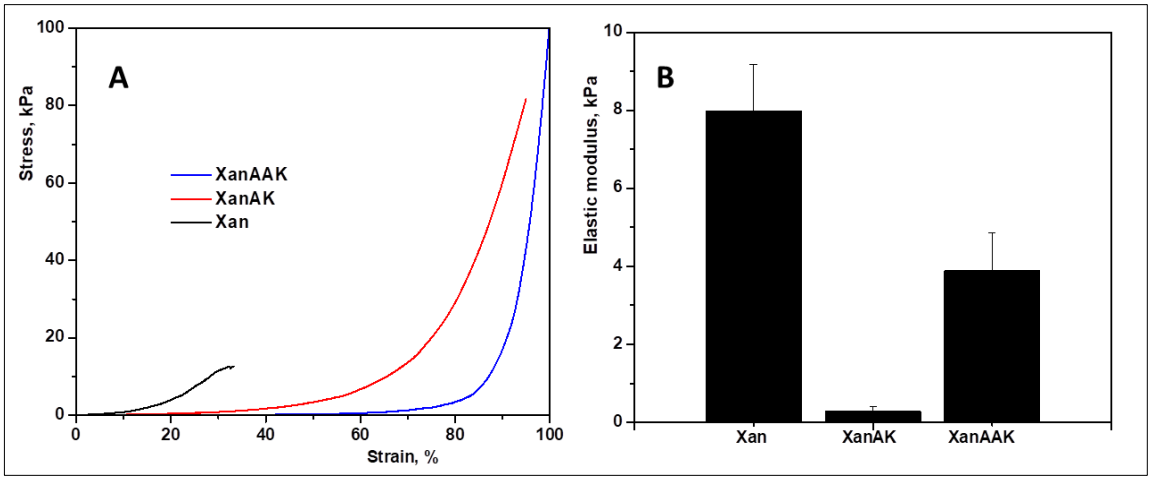

Figure 4. (A) Stress-strain profiles for Xan hydrogel films, XanAK, and XanAAK patches(B). The values of elastic modulus determined for each sample as the gradient of the initial linear portion in the stress-strain curve

The stress-strain profile for swollen Xan hydrogel films (Figure 4A) supports also the weak mechanical properties of this sample, in which cracks were developed after 30% strain. By contrast, the XanAK and XanAAK patches were very stable against the mechanical forces applied, which indicates that the plasticization effect of water didn't affect the compressive properties of the Xan-based patches. The increase of the patches stiffness is further supported by the values of the elastic moduli, which are lower for Xan-based patches (Figure 4B).

3.4. *In vitro* release of amoxicillin and ketoprofen from Xan/XanA patches

The concept of drug release refers to the migration of drugs from within a polymer matrix to the surface of the base material and its release at a more or less constant rate in the environment in which it was placed. This process is profoundly influenced by a number of factors such as drug solubility, ionic charge, the structure of the release medium and its permeability, the interaction of the drug with the polymer matrix, etc.

On the other hand, the mathematical modeling of the release profile of drugs is important both theoretically and practically because it allows the comparative evaluation of release systems and the calculation of kinetic parameters [31]. All of these offer the possibility of evaluation and subsequent control of the properties of the basic matrix according to the proposed specifications.

The release data of the active substances for the tested materials (XanAK and XanAAK) clearly show the difference between the two systems (Figure 5).

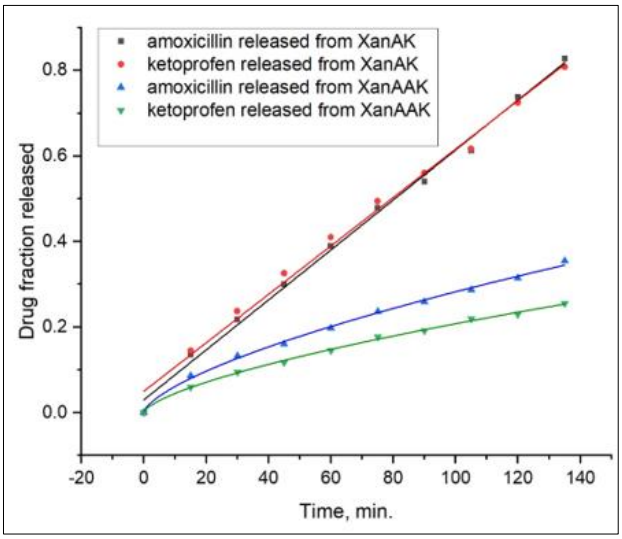

Figure 5. Fraction of drugs released over time for XanAK and XanAAK

The release of the active principles from XanAK follows a zero kinetics (Table 1) while the system consisting of XanAAK is best described by the Korsmeyer-Peppas model [32,33].

Mathematical models:

Zero order kinetics - According to this model, drug release from the dosage form can be represented by the equation:

$$Q(t) = A + Bt \quad (2)$$

where: Q(t) – amount of drug released at time t, B – rate constant and A – free parameter.

Korsmeyer-Peppas model describes the drug release from a polymeric matrix and it is represented by the following equation:

$$\frac{M_t}{M_0} = k \times t^n \quad (3)$$

where M_t/M_0 represents the fraction of the drug released at time t, M_t and M_0 are the amount of drug released at time t and the initial amount of drug used, k is rate constant incorporating the characteristics of the delivery system and n is the release exponent, which is indicative of the release mechanism.

A value of n = 0.5 indicates a Fickian diffusion mechanism of the drug from the inside of the material, while a value $0.5 < n < 1$ indicates a non-Fickian behavior.

Table 1 summarizes the kinetic parameters obtained for the tested materials according to the two models presented above.

Table 1. Kinetic parameters for drug release experiments

Model	Sample	Parameters		
Zero order		**A**	**B**	**R^2**
	XanAK /amoxicillin	0.0298	0.0584	0.995
	XanAK / ketoprofen	0.0499	0.0566	0.991
Korsmeyer-Peppas		**k**	**n**	**R^2**
	XanAAK / amoxicillin	0.0132	0.664	0.997
	XanAAK / ketoprofen	0.0096	0.666	0.998

Unchanged xanthan capsules release the two bioactive components at almost the same rate, but after about 140 minutes the entire structural edifice collapses. The conclusion is that this formulation cannot constitute a controlled release system.

Acrylic acid-modified xanthan capsules maintain their structural integrity. The rate of drug release is slow and selective (Figure 4., Table 1). In all cases, amoxicillin is released at a slightly faster rate than ketoprofen, due to the structural differences of the drugs and the different capacities to interact with the polymer matrix for the two materials.

3.5. Anti-inflammatory activity for XanAA/XanAAK materials

The anti-inflammatory activity of the patches is given by the presence in their composition of ketoprofen. The results of the *in vitro* testing of this capacity are summarized in Table 2.

Table 2. *In vitro* anti-inflammatory activity for the tested materials

Sample	Ketoprofen in sample, mg	Inhibition, %
Reference	20	61.27 ± 0.021
XanAK	20	57.8 ± 0.062
XanAAK	20	38.64 ± 0.057

The patches have anti-inflammatory activity but, as expected, it is lower than in the case of the reference, because there is dependence on the contact time factor. The materials were designed for the slow release of drugs over time.

3.6. Antimicrobial activity

The addition of amoxicillin to the biomaterials influenced their antimicrobial properties. XanAK and XanAAK show the same biocidal capacity, after 24 h, against microorganisms that have been tested with one exception, the bacterium *E. coli*. For this microorganism the best activity is presented only by the biomaterial XanAAK, with an inhibition capacity of 77% (Table 3).

Table 3. Antimicrobial activity for the tested materials

Sample	CFU	CFU	Inhibition, %	CFU	CFU	Inhibition, %	CFU	CFU	Inhibition, %
	100 μL	100 μL		100 μL	100 μL		100 μL	100 μL	
	Candida albicans ATCC 90028			*Staphylococcus aureus* ATCC 25923			*Escherichia coli* ATCC 25922		
	Initial number of colonies	after 24 h		Initial number of colonies	after 24 h		Initial number of colonies	after 24 h	
Reference	255	255		293	293		287	287	0
XanAK	255	0	100	293	0	100	287	139	52
XanAAK	255	0	100	293	0	100	287	66	77

CFU= Colony-forming Units

3.7. Materials' morphology

SEM images (Figure 6) offer more insights about the morphology of XanAK and XanAAK patches. The chemical modification of xanthan by esterification with acrylic acid gives it a compact and fine surface (Figure 6b) which is reflected in the retard characteristics of drugs release.

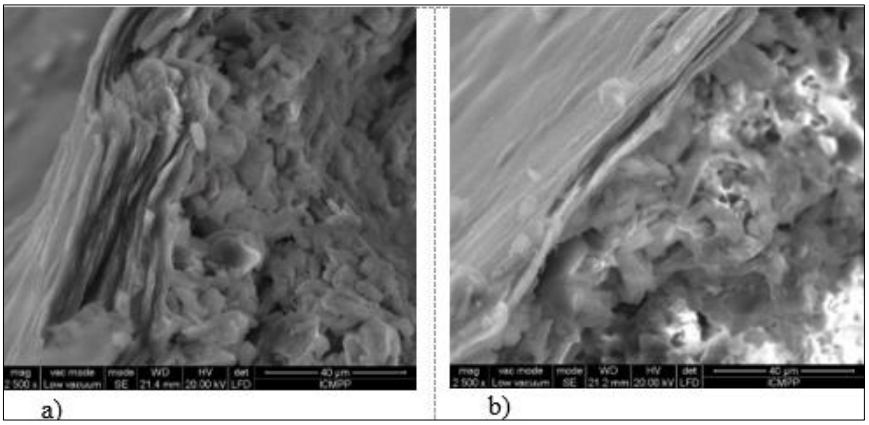

Figure 6. SEM micrographics for XanAK (a) and XanAAK (b)

4. Conclusions

A new drug delivery system based on xanthan was obtained by esterification of the named polysaccharide with acrylic acid. Formulations containing amoxicillin and ketoprofen were developed and analyzed.

Mechanical strength tests showed a substantial improvement in the resilience and flexibility of the polysaccharide matrix modified by esterification. The release of bioactive substances from the basic matrix follows a Korsmeyer-Peppas type kinetics with a non-Fickian behavior. The modified xanthan-based transport system was shown to be antimicrobial active with an inhibition rate of almost 100% on gram-positive and gram-negative bacteria.

In summary, the obtained results confirm that the prepared xanthan-based material could be promising carrier for release of bioactive compounds with potential medical and cosmetic applications. As a perspective, we are considering the integration of bioactive substances with anti-cellulite action (cosmetic applications) in the polymer matrix that proves it has mechanical strength, flexibility and can act as a biocompatible transdermal drug delivery system.

Acknowledgments: The PN-III-P1-1.1-TE-2016-1697 project [TE117/10.10.2018] is gratefully acknowledged

References

1. ANGHEL, N., Lignin and polyphenols from vegetal wastes as key modulators of metabolic pathways during plant development, *Cellulose Chem. Technol.*, **50**(9-10), 2016, 967–971.
2. AGUIAR, A.E., DE O. SILVA, M., RODAS, A.C.D., BERTRAN, C.A., Mineralized layered films of xanthan and chitosan stabilized by polysaccharide interactions: A promising material for bone tissue repair topical applications or drug delivery systems, *Carbohydr. Polym.*, **207**, 2019, 480–491. https://doi.org/10.1016/j.carbpol.2018.12.006
3. MERLUSCA, I.P., IBANESCU, C., TUCHILUS, C., DANU, M., ATANASE, L.I., POPA, I.M., Characterization of neomycin-loaded xanthan-chitosan hydrogels for topical applications, *Cellulose Chem. Technol*., **53**(7-8), 2019, 709–719. https://doi.org/10.35812/CelluloseChemTechnol.2019.53.69
4.CAI, X.J., MESQUIDA, P., JONES, S.A., Investigating the ability of nanoparticle-loaded hydroxypropyl methylcellulose and xanthan gum gels to enhance drug penetration into the skin, *Int. J. Pharm*., **513**, 2016, 302–308. https://doi.org/10.1016/j.ijpharm.2016.08.055

5. MISHRA, B., SAHOO, S.K., SAHOO, S., Liranaftate loaded Xanthan gum based hydrogel for topical delivery: Physical properties and ex-vivo permeability, *Int. J. Biol. Macromol*., **107**, 2018, 1717–1723. https://doi.org/10.1016/j.ijbiomac.2017.10.039
6. KOOP, H.S., FREITAS, R.A., SOUZA, M.M., SAVI-JR., R., SILVEIRA, J.L.M., Topical curcumin-loaded hydrogels obtained using galactomannan from *Schizolobiumparahybae* and xanthan, *Carbohydr. Polym*., **116**, 2015, 229–236. https://doi.org/10.1016/j.carbpol.2014.07.043
7. BUENO, P.V.A., HILAMATU, K.C.P., CARMONA-RIBEIRO, A.M., PETRI, D.F.S., Magnetically triggered release of amoxicillin from xanthan/ Fe3O4/albumin patches, *Biol. Macromol.*, **115**, 2018, 792–800. https://doi.org/10.1016/j.ijbiomac.2018.04.119
8. COVIELLO, T., TROTTA, A.M., MARIANECCI, C., CARAFA, M., DI MARZIO, L., RINALDI, F., DI MEO, C., ALHAIQUE, F., MATRICARDI, P., Gel-embedded niosomes: Preparation, characterization and release studies of a new system for topical drug delivery, *Colloid Surface B*, **125**, 2015, 291–299. https://doi.org/10.1016/j.colsurfb.2014.10.060
9. HANNA, D.H., SAAD, G.R., Encapsulation of ciprofloxacin within modified xanthan gum- chitosan based hydrogel for drug delivery, *Bioorg. Chem*., **84**, 2019, 115–124.
http://doi.org/10.1016/j.bioorg.2018.11.036
10. HONGA, Y., YANG, J., LIU, W., GU, Z., LI, Z., CHENG, L., LI, C., DUAN, X., Sustained release of tea polyphenols from a debranched corn starch–xanthan gum complex carrier, *LWT-Food Sci. Technol.*, **103**, 2019, 325–332. https://doi.org/10.1016/j.lwt.2019.01.014
11. ZHENG, Z., LIAN, F., ZHU, Y., ZHANG, Y., LIU, B., ZHANG, L., ZHENG, B., pH-responsive poly (xanthan gum-g-acrylamide-g-acrylic acid) hydrogel: Preparation, characterization, and application, *Carbohydr. Polym.*, **210**, 2019, 38–46. https://doi.org/10.1016/j.carbpol.2019.01.052
12. SABAA, M.W., ELELLA, M.H.A., HANNA, D.H., MOHAMED, R.R., Encapsulation of bovine serum albumin within novel xanthan gum based hydrogel for protein delivery, *Mater. Sci. Eng. C*, **94**, 2019, 1044–1055. https://doi.org/10.1016/j.msec.2018.10.040
13. JAIPAL, A., PANDEY, M.M., ABHISHEK, A., VINAY, S., CHARDE, S.Y., Interaction of calcium sulfate with xanthan gum: Effect on *in vitro* bioadhesion and drug release behavior from xanthan gum based buccal discs of buspirone, *Colloid Surface B***, 111**, 2013, 644–650.
https://doi.org/10.1016/j.colsurfb.2013.06.052
14. ANGHEL, N., LAZAR, S., CIUBOTARIU, B.I., VERESTIUC, L., SPIRIDON, I., New cellulose-based materials as transdermal transfer systems for bioactive substances, *Cellulose Chem. Technol*., **53**(9-10), 2019, 879. https://doi.org/10.35812/CelluloseChemTechnol.2019.53.85
15. FANTOU, C., COMESSE, S., RENOU, F., GRISEL, M., Impact of backbone stiffness and hydrophobic chain length of modified xanthan on oil in water emulsion stabilization, *Carbohydr. Polym.*, **216**, 2019, 352–359. https://doi.org/10.1016/j.carbpol.2019.03.079
16. TOLEDO, P.V.O., PETRI, D.F.S., Hydrophilic, hydrophobic, Janus and multilayer xanthan based cryogels, *Int. J. Biol. Macromol.*, **123**, 2019, 1180–1188. https://doi.org/10.1016/j.ijbiomac.2018.11.193
17. JIANG, H., DUAN, L., REN, X., GAO, G., Hydrophobic association hydrogels with excellent mechanical and self healing properties, *Eur. Polym. J.*, **112**, 2019, 660–669.
https://doi.org/10.1016/j.eurpolymj.2018.10.031
18. SAHOO, D., SARKAR, S., JANA, S., A simple synthesis of ketone from carboxylic acid using tosyl chloride as an activator, *Tetrahedron Lett*., **60**, 2019, 151084.
https://doi.org/10.1016/j.tetlet.2019.151084
19. CHETOUANI, A., ELKOLLI, M., BOUNEKHEL, M., BENACHOUR, M., Chitosan/oxidized pectin/PVA blend film: mechanical, and biological properties, *Polymer Bulletin*, **74**, 2017, 4297–4310. https://doi.org/10.1007/s00289-017-1953-y
20. GUNATHILAKE, K.D.P.P., RANAWEERA, K.K.D.S., RUPASINGHE, H.P.V., *In Vitro* Anti-Inflammatory Properties of Selected Green Leafy Vegetables, *Biomedicines*, **6**, 2018, 107–117. https://doi.org/10.3390/biomedicines6040107

21. ANYASOR, G.N., OKANLAWON, A.A., OGUNBIYI, B., Evaluation of anti-inflammatory activity of *Justiciasecunda Vahl* leaf extract using *in vitro* and in vivo inflammation models, *Clin. Phytosci*., **5**, 2019. https://doi.org/10.1186/s40816-019-0137-8
22. CHANDRA, S., CHATTERJEE, P., DEY, P., BHATTACHARYA, S., Evaluation of *in vitro* anti-inflammatory activity of coffee against the denaturation of protein, *Asian Pac. J. Trop. Biomed*., **2**, 2012, 178–180. https://doi.org/10.1016/S2221-1691(12)60154-3
23.SUFLET, D.M., PELIN, I.M., DINU, M.V., LUPU, M., POPESCU, I., Hydrogels based on monobasic curdlan 415 phosphate for biomedical applications. *Cellulose Chem. Technol*., **53**, 2019, 897–906. https://doi.org/10.35812/CelluloseChemTechnol.2019.53.87
24. RINAUDO, M., MILAS, M., LAMBERT, F., VINCENDON, M., Proton and carbon-13 NMR investigation of xanthan gum, *Macromol.*, **16**, 1983, 816–819. https://doi.org/10.1021/ma00239a018
25.NEJADMANSOURI, M., SHAD, E., RAZMJOOEI, M., SAFDARIANGHOMSHEHA, R., DELVIGNE, F., KHALESI, M., Production of xanthan gum using immobilized *Xanthomonas campestris* cells: Effects of support type, *Biochem. Eng. J.*, **157**, 2020, 107554.
http://doi.org/10.1016/j.bej.2020.107554
26. SARA, H., YAHOUM, M.M., LEFNAOUI, S., ABDELKADER, H., MOSTEFA, N.M., New alkylated xanthan gum as amphiphilic derivatives: Synthesis, physicochemical and rheological studies, *J. Mol. Struct.*, **1207**, 2020, 127768. https://doi.org/10.1016/j.molstruc.2020.127768
27. WANG, Z., WU, J., ZHU, L., ZHAN, X., Characterization of xanthan gum produced from glycerol by a mutant strain *Xanthomonas campestris* CCTCC M2015714, *Crbohydr. Polym.*, **157**, 2017, 521–526.
https://doi.org/10.1016/j.carbpol.2016.10.033
28. FANTOU, C., ROY, A.N., DÉ, E., COMESSE, S., GRISEL, M., RENOU, F., Chemical modification of xanthan in the ordered and disordered states: An open route for tuning the physico-chemical properties, *Carbohydr. Polym.*,**178**, 2017, 115–122.
https://doi.org/10.1016/j.carbpol.2017.09.039
29. HAMCERENCU, M., DESBRIERES, J., POPA, M., KHOUKH, A., RIESS, G., New unsaturated derivatives of Xanthan gum: Synthesis and characterization, *Polymer*, 48, 2007, 1921-1929. https://doi.org/10.1016/j.polymer.2007.01.048
30. TROMBINO, S., SERINI, S., CASSANO, R., CALVIELLO, G., Xanthan gum-based materials for omega-3 PUFA delivery: Preparation, characterization and antineoplastic activity evaluation, *Carbohydr. Polym.*, **208**, 2019, 431–440. https://doi.org/10.1016/j.carbpol.2019.01.001
31. GOUDA, R., BAISHYA, H., QING, Z., Application of Mathematical Models in Drug Release Kinetics of Carbidopa and Levodopa ER Tablets, *J. Develop. Drugs.*, **6**, 2017, 171.
https://doi.org/10.4172/2329-6631.1000171
32. MHLANGA, N., RAY, S.S., Kinetic models for the release of the anticancer drug doxorubicin from biodegradable polylactide/metal oxide-based hybrids, *Int. J. Biol. Macromol*., **72**, 2015, 1301–1307. http://dx.doi.org/10.1016/j.ijbiomac.2014.10.038
33. PANOTOPOULOS, G.P., HAIDAR, Z.S., Mathematical Modeling for Pharmaco-Kinetic and -Dynamic Predictions from Controlled Drug Release Nano Systems: A Comparative Parametric Study, Sci. (*Hindawi*, Online), 2019. https://doi.org/10.1155/2019/9153876

Manuscript received: 25.09.2020